Core level studies of calcite and dolomite

Järvinen, Lauri; Leiro, Jarkko; Heinonen, Markku

[Link to publication](#)

Core level studies of calcite and dolomite

Lauri Järvinen,[a]* Jarkko Leiro[b] and Markku Heinonen[b]

Conventional X-ray photoelectron spectroscopy (XPS) and synchrotron-based X-ray photoelectron spectroscopy (HRXPS) have been used to study Iceland spar calcite ($CaCO_3$) and dolomite ($CaMg(CO_3)_2$). The obtained full widths at half maximum (FWHMs) are mostly narrower than in the previous results, which together with the symmetry of the fitted peaks indicate effective neutralisation of surface charging. Some previously unidentified features observed in the Ca 2p, C 1s and O 1s spectra of calcite have been suggested to be bulk plasmons. Also, surface core level shifts in Ca 2p (in calcite) and Mg 2p (in dolomite) spectra have been obtained and found to be consistent between XPS and HRXPS measurements. A peak attributed to carbide (CaC_2) has been suggested to indicate beam-assisted interaction with hydrocarbons found on the surface. Copyright © 2014 John Wiley & Sons, Ltd.

Introduction

Calcite ($CaCO_3$) is the main mineral constituting limestone and fairly common around the earth in a multitude of mineralogical environments. Dolomite ($CaMg(CO_3)_2$) is also often present in limestones, which are widely used as raw materials in various desulfurisation processes of flue gases from power plants utilising coal combustion.[1] Other large scale applications include, for example, the use as filler in paper and cement as well as in soil improvement. An environmental aspect of calcite and dolomite lies in their role in the global carbon dioxide cycle.[2,3] X-ray photoelectron spectroscopy (XPS) can provide useful information concerning the chemical bonding of calcite and dolomite surfaces for better understanding of, for example, chemical reactions taking place in flue gas desulfurisation or environmental processes.

Calcite (space group $R\bar{3}c$) has a rhombohedral crystal structure. It consists of alternating layers of calcium (Ca^{2+}) and carbonate (CO_3^{2-}) ions that are perpendicular to the crystallographic *c*-axis. Each calcium ion is coordinated to six oxygen atoms. The coplanar vectors a and b of the calcite unit cell have the same length of 0.499 nm and an angle of 120° between them, while the perpendicular *c*-axis is 1.706 nm long.[4] Iceland spar is a transparent and colourless variety of calcite with a strong double refraction.[5]

Dolomite is also a rhombohedral carbonate mineral with slightly lower symmetry (space group $R3$). The difference to the calcite crystal structure is that every other Ca^{2+} layer is replaced by magnesium (Mg^{2+}) ions.[6–8] The lattice parameters of a = b = 0.488 nm and c = 1.629 nm have been reported.[9] Dolomite is a solid-solution mineral, which means that the Mg/Ca relation can vary. In other words, calcium and magnesium can substitute each other in the mineral lattice. If there is no magnesium, the mineral is called calcite ($CaCO_3$); if there is no calcium, the mineral is called magnesite ($MgCO_3$).

In XPS, the surface of a sample is irradiated with X-rays. As a result, a series of photoelectrons are emitted leaving behind a positive charge, which requires neutralisation if the sample has a large band gap (i.e. the sample is an insulator such as calcite and dolomite).[10] The values of indirect electronic band gaps of dolomite and calcite have been reported to be 5.0 and 6.0 eV,[9,11] respectively. Especially in the case of synchrotron radiation, charging on the surface distorts and widens the photoelectron peaks, thus making it more difficult to identify the subtle details in the chemical

environment of the sample surface. In addition, surface charging also causes false shifts in binding energies that hinder the identification of the correct binding energy of a peak in a spectrum.[12–16]

Recently, it has been shown that it is possible to measure XPS spectra of insulators with no charge broadening,[17] which is promising for the study of non-conducting solids. To the authors' knowledge, no calcite nor dolomite spectra (with an exception of the findings of Doyle *et al.*,[18] in which case, CaO reacted with CO_2 and produced $CaCO_3$) have been measured previously with synchrotron-based XPS. Energy loss satellites in the Ca 2p spectra of calcite have been observed,[19–21] but no interpretations of their origins have been presented in these publications. Interestingly, it was possible to experimentally identify the plasmon energies of calcite that can be extracted from the results of the density functional theory (DFT) calculations by Medeiros *et al.*[22] It turned out, that their optical physics calculations of collective excitations are consistent with our experimental results. Because the value of zero for the real part of the dielectric function predicts collective excitations of electrons (i.e. bulk plasmons), that are readily observable in XPS data, an experimental comparison with the calculations is possible. In this study, we have utilised both synchrotron-based high-resolution XPS (HRXPS) and conventional XPS to measure core level spectra of a single crystal Iceland spar calcite and a metamorphic (physically and/or chemically altered because of high temperature and/or high pressure conditions) polycrystalline dolomite from Reetinniemi, Finland.

Experimental

HRXPS

The synchrotron-based high-resolution measurements were carried out at beamline I411 of MAX II synchrotron laboratory in Lund, Sweden. The beamline is equipped with a modified

*   *Correspondence to: L. Järvinen, Geology and Mineralogy, Department of Natural Sciences, Åbo Akademi University, Åbo, Finland. E-mail: lauri.jarvinen@abo.fi*

a   *Geology and Mineralogy, Department of Natural Sciences, Åbo Akademi University, Åbo, Finland*

b   *Department of Physics and Astronomy, University of Turku, Turku, Finland*

SX-700 monochromator (Carl Zeiss, Oberkochen, Germany) and a hemispherical Scienta R4000 (Scienta Scientific AB, Uppsala, Sweden) electron energy analyser. The pressure was of the order of 10^{-8} mbar. The overall instrumental energy resolutions were 0.1, 0.2 and 0.4 eV for photon energies of 400, 550 and 780 eV, respectively. The electron take-off angles (measured from the sample surface) were equal to 45°. The spectrometer was calibrated using Au $4f_{7/2}$ and Ag $3d_{5/2}$ photoelectron lines at 84.0 and 368.3 eV, respectively. In addition, the Fermi level of gold was used for calibration.

Both calcite and dolomite samples were mounted into a sample holder with integrated dipole type electron flood gun and cleaved in the vacuum chamber. For the measurement of Ca 2p spectrum of calcite, a conductive mask[23] made of gold was placed on top of the sample to improve surface neutralisation. The mask was grounded, and it had a 2-mm hole to limit the measurement area, thus making it easier to control the experiment. The conductive copper substrate was also grounded for all experiments.

The obtained spectra were analysed with Igor Pro 5.02 (WaveMetrics Inc, OR, USA) software and a special macro package.[24] A Shirley background correction method and a Gaussian–Lorentzian (Voigt) peak shape were used unless otherwise stated. In the case of calcite, the peak positions were calibrated using the studies of Järvinen *et al.* and Blanchard and Baer.[25,26] For the Ca 2p spectra (also for those obtained with conventional XPS), the spin-orbit splitting $\Delta_{s-o} = 3.6$ eV and the peak intensity ratio of 1:2 were used. The lifetime widths were fixed to 0.17 eV.[27]

Conventional XPS

Conventional XPS measurements with non-monochromatic Mg K_α and monochromatic Al K_α radiation were carried out with a PHI 5400 spectrometer (Physical Electronics, MN, USA). The corresponding powers of the X-ray source were 200 and 300 W, respectively. The wide scan survey spectrum (Fig. 1) was measured with Mg K_α X-rays. The overall instrumental energy resolution was 0.9 eV in the case of non-monochromatic radiation and 0.7 eV in the case of monochromatic radiation. The electron take-off angles (measured from the sample surface) are noted in the figures or their captions. The pressure was of the order of 10^{-9} mbar. In the case of monochromatic Al K_α excitation radiation, an electron flood gun was used for

charge neutralisation, whereas for Mg K_α, electrons emitted from an aluminium window of the X-ray tube were used to compensate for charging. The calcite sample was cleaved in the vacuum chamber.

Results and discussion

Identification of the studied surfaces

X-ray diffraction (XRD) patterns showed that the calcite was cleaved along the ($10\overline{1}4$) surface. In addition, a minor peak referring to ($20\overline{2}6$) surface was observed. The XRD-spectrum of the cleaved polycrystalline dolomite sample showed ($10\overline{1}4$), ($01\overline{1}2$) and ($\overline{1}\overline{1}26$) reflections, for which the first one was clearly dominant.

HRXPS of calcite

Surface core level shifts

Figure 2 shows two high-resolution Ca 2p spectra of Iceland spar recorded with photon energies 550 and 780 eV. The Ca $2p_{3/2}$ binding energy of 346.7 eV[26] was used for calibration of the peak positions. The lifetime widths were fixed to the calculated value of 0.17 eV for Ca 2p,[27] which is in agreement with X-ray emission measurements of metallic calcium.[28] For both bulk and surface components of the Ca 2p spectra, the instrumental widths were allowed to change. The Gaussian widths of the fitted spectra varied between 1.0 and 1.3 eV, which include both instrumental and phonon broadening. Two Ca 2p doublets with
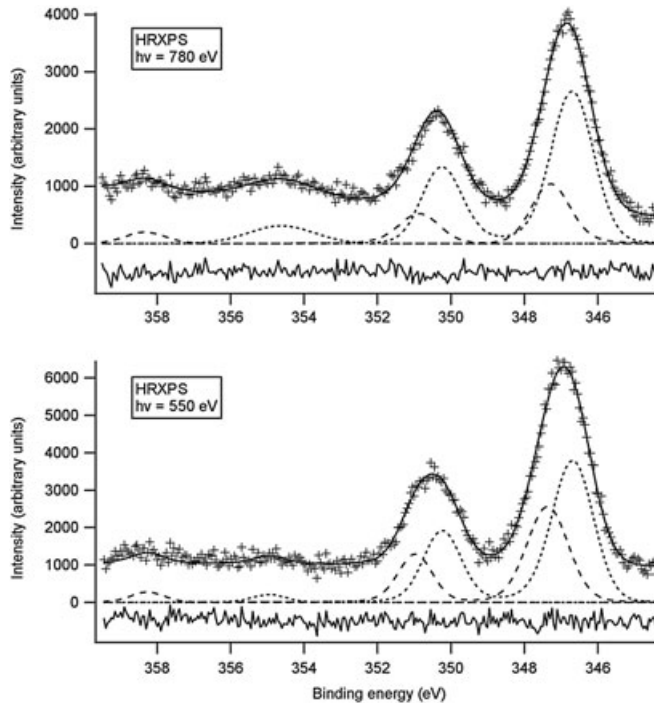
Figure 2. Ca 2p spectra of Iceland spar calcite obtained with synchrotron-based high-resolution XPS (HRXPS). Markers indicate raw data without background subtraction, dashed lines are the fitted individual components and the thin solid line behind the markers is the sum of the dashed lines. The horizontal solid line below the peaks shows the differences between the raw data and the sum of the fitted components, that is, the residues. The electron take-off angle was 45°. A linear background subtraction method was used.
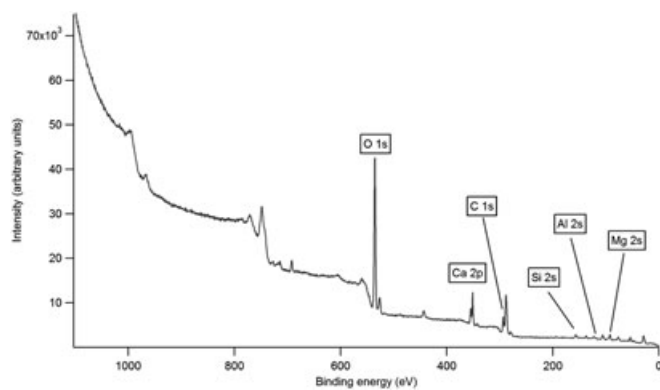
Figure 1. A survey spectrum of a polycrystalline dolomite ($CaMg(CO_3)_2$) from Reetinniemi, Finland. The spectrum was recorded from a powder sample. The electron take-off angle was 45°.

a separation of 0.7 eV can be fitted for both spectra. Two satellite features fitted in Fig. 2 occur at about 8 eV higher binding energies than Ca 2p$_{1/2}$ and Ca 2p$_{3/2}$ peaks.

Calcite has good cleavage properties along the (10$\bar{1}$4) surface partly because no strongly covalent C–O bonds and the least amount of ionic Ca–O bonds are broken.[29,30] The creation of a fresh surface leads to a removal of one oxygen atom; on the (10$\bar{1}$4) surface, each Ca^{2+} ion is coordinated to five nearest-neighbour oxygen atoms instead of six in the bulk.[31] The doublet on the high binding energy side in the Ca 2p spectra in Fig. 2 is suggested to originate from surface Ca atoms. This separation of peaks in binding energy is called surface core level shift (SCLS).[32] In the initial state of the XPS process, an increase of the binding energy of electrons in the case of cations at the surface can be largely explained by the surface Madelung potential,[33] because the surface Madelung constant is often smaller than the bulk one. According to the Mönch's model,[34] an assumption of a constant anion-cation distance leads to SCLS being proportional to the difference between bulk and surface Madelung constants.

In addition, screening of the created core hole by the valence electrons (final state effect) has an influence on the binding energy of an emitted photoelectron. There are more electrons around calcium in the bulk than in the surface. Therefore, the binding energy of the surface Ca 2p core level is reduced more than the corresponding energy of the bulk 2p level, and the magnitude of the SCLS decreases because of screening. According to Veal and Paulikas,[35] who studied screening in CaF$_2$ (an ionic compound with an experimental band gap of 12.1 eV[36]), the screening of the Ca 2p core hole should be local. They reached this conclusion by applying the Z + 1 approximation, in which (for outer electrons) an ion that has atomic number Z and a deep core hole is treated as if it were a neutral atom in its ground state with atomic number Z + 1. Therefore, Ca^{2+}, after losing a core electron, should closely resemble Sc^{2+} ion.[35]

The SCLS of 0.7 ± 0.1 eV, which was also observed in the Ca 2p spectra obtained with both non-monochromatic Mg K$_{\alpha}$ (not shown) and monochromatic Al K$_{\alpha}$ (Fig. 3, Fig. 4 and later text) X-rays, is substantially smaller than that of the previously reported value of 1.3 ± 0.2 eV.[19] If smaller number of Ca–O bonds is the dominating factor behind larger binding energy shifts, it could be that in the referred case,[19] the coordination of Ca^{2+} by oxygen was even lower than in our case. This might be caused by different amount of steps, kinks and edges on the surface that lead to a different number of Ca–O bonds and hence a different SCLS.

Satellite features

Two satellite features have been fitted into Fig. 2 for both 550 and 780 eV photon energies. They occur at about 8 eV from Ca 2p$_{1/2}$ and Ca 2p$_{3/2}$ components. These four satellites are suggested to be caused by plasmons originating from the bulk. Their energies are in accordance with a previously measured reflection electron energy loss spectrum of calcite[11] and previously measured conventional XPS spectra of calcite.[19] In addition, DFT calculations of the calcite dielectric function $\varepsilon(\omega)$, which was published by Medeiros *et al.*,[22] support our suggestion. By using the interpretation given by Leiro, Minni and Suoninen,[37] the equation Re $\varepsilon(\omega_p) = 0$ gives the frequency value ω_p of a bulk plasmon (occurring at approximately 8 eV in the DFT calculations), while in the case of Re $\varepsilon(\omega_s) = -1$, the frequency ω_s of a surface plasmon is given (occurring at approximately 7.5 eV in the DFT calculations). By showing that Im $\varepsilon(\omega)$ has a local
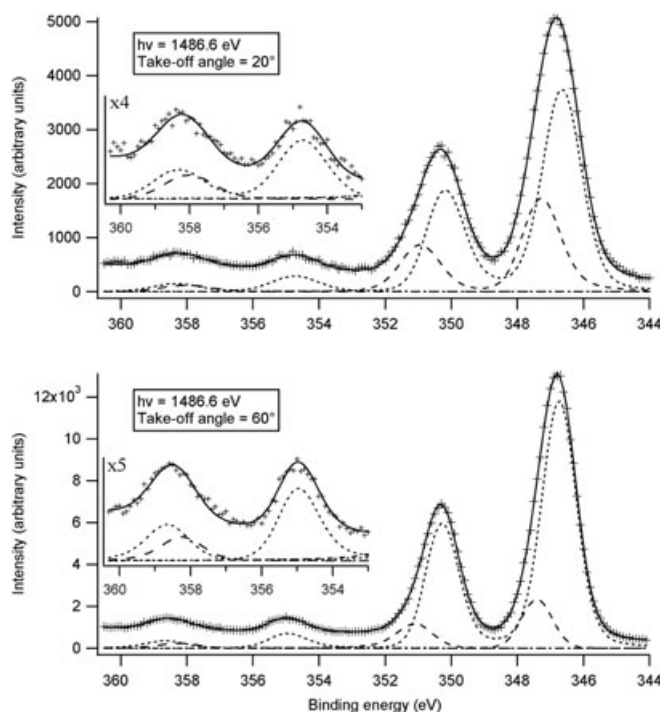

Figure 3. Ca 2p spectra of Iceland spar obtained with conventional XPS. Fourfold and fivefold enlargements (of the vertical axes) of the satellite regions are shown for upper and lower panels, respectively. Markers indicate raw data without background subtraction, dashed lines are the fitted individual components and the thin solid line is the sum of the dashed lines. The photoelectron take-off angles have been set to 20° and 60° (measured from the sample surface). A linear background subtraction method was used.

minimum at approximately 8 eV, Medeiros *et al.*[22] show that damping of the satellite is smaller around this energy. At approximately 7 eV, the real part of the dielectric function has another zero point, but the damping part is clearly higher. This can explain why there are no peaks in Fig. 2 at about 7 eV higher binding energies from the Ca 2p doublet.

In the case of $hv = 550$ eV, a larger proportion of the measured signal originates from the surface, and therefore, the surface plasmons have a larger contribution to the total spectrum, which can be seen as less pronounced energy loss features. From the data presented by Medeiros *et al.*,[22] it can be deduced that the energy difference between surface and bulk plasmon would be about 0.5 eV. In addition, the data of Medeiros *et al.*[22] indicate that there are bulk plasmons also at about 11.5 eV higher binding energies than the Ca 2p doublet. If the satellites occurring at around 8.0 and 11.5 eV from the Ca 2p$_{1/2}$ and Ca 2p$_{3/2}$ components are considered (as they are in Fig. 4), it would be seen that the satellite peak located at about 8 eV from the Ca 2p$_{1/2}$ peak consists of two features. The other component comes from the Ca 2p$_{3/2}$ main line.

Full widths at half maximum

The full widths at half maximum (FWHM) of the fitted Ca 2p peaks in Fig. 2 are all between 1.0 and 1.3 eV. Previous results obtained with conventional XPS (non-monochromatic Mg K$_{\alpha}$ or monochromatic Al K$_{\alpha}$ excitation) range from 1.3 to 2.0 eV,[19–21,25,38] which indicates that our reduction of charge related broadening has been effective. However, no surface component was resolved by Baer and Moulder, Gopinath et al., Järvinen et al. and Ni and
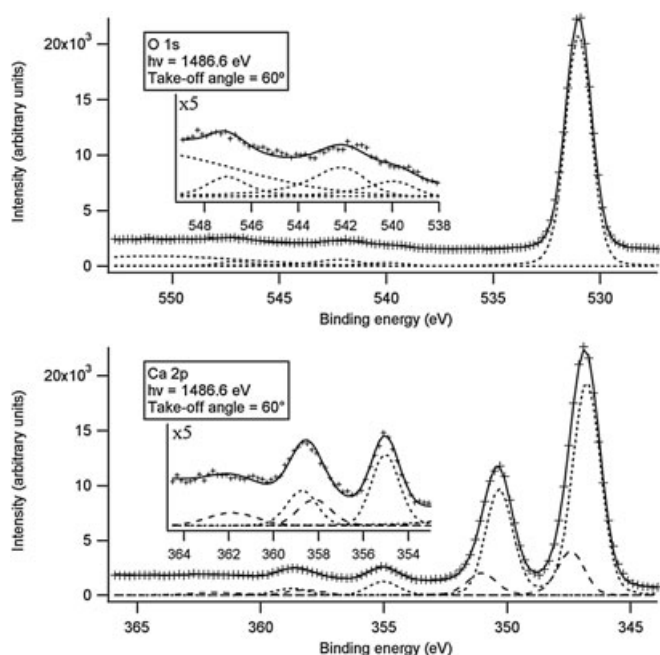
Figure 4. Conventional XPS spectra of O 1s and Ca 2p. Fivefold enlargements (of the vertical axes) of the satellite regions are shown. In the O 1s spectrum, three satellites are found at approximately 8.7, 11.0 and 16.1 eV higher binding energies than the main carbonate peak. We suggest that the first and second energy loss features are bulk plasmons because of the consistency with the DFT calculations by Medeiros *et al.*[22] The third feature might be to some extent contributed by a second order plasmon because its energy is approximately twice as large as the energy of the first feature. In the Ca 2p spectrum, it can be seen that the satellites actually consist of two doublets located at 8.3 and 11.5 eV higher binding energies than the Ca 2p bulk doublet. Using the same interpretation as previously, we suggest that these satellites are bulk plasmons. Markers indicate raw data without background subtraction, dashed lines are the fitted individual components and the thin solid line is the sum of the dashed lines. A linear background subtraction method was used in the fitting procedure of the Ca 2p spectrum.

Ratner.[20,21,25,38] If there is an unresolved peak in these spectra, it could help to explain the large width of the peaks. Another aspect that might reduce the FWHM is that our sample was cleaved in vacuum where there are fewer possibilities for creation of new chemical bonds that would increase the FWHM. In the case of narrower FWHMs, the SCLSs and the satellite features become better resolved. With a conventional XPS, monochromatic X-ray source has been reported to cause unstable sample charging on the calcite surface that resulted in peak broadening.[19] In addition, electron irradiation has been reported to cause decomposition.[39]

Conventional XPS

Take-off angle in Ca 2p spectrum

Figure 3 shows two Ca 2p spectra obtained with monochromatic radiation and take-off angles (measured from the sample surface) of 20° and 60°. Fourfold and fivefold enlargements (of the vertical axes) of the satellite regions are shown for the upper and lower panel, respectively. Shoulders on the high binding energy side are interpreted to represent SCLSs, which appear at 0.7 ± 0.1 eV higher binding energies. The surface sensitivity of the smaller

take-off angle can be well observed as a stronger surface related peak in the upper spectrum. The binding energy shifts are in agreement with the SCLSs observed with synchrotron radiation. Also, FWHMs are equal to 1.3 ± 0.1 eV.

Two satellite features are located at 8.2 ± 0.1 eV higher binding energies measured from the Ca 2p peaks, which is also in reasonable agreement with our high-resolution measurements. Further agreement with the interpretations presented above of the DFT calculations[22] suggests that the features are bulk plasmons. In the more surface sensitive case of 20° take-off angle (Fig. 3), the plasmons have 0.2 eV smaller energies when compared with the case of 60° take-off angle. This supports the previous discussion of approximately 0.5 eV energy difference between bulk and surface plasmons. The difference in plasmon energies is interpreted to be caused by a more pronounced surface plasmon in the 20° take-off angle spectrum. Also, a third satellite peak, which is located at about 11.4 eV higher binding energy measured from the Ca $2p_{3/2}$ peak, is fitted in the figure (see Fig. 4 and Section on O 1s and Ca 2p Spectra for the discussion).

Take-off angle in C 1s spectrum

The same change of the take-off angle from 20° to 60° was used to measure the C 1s spectrum. The results obtained with non-monochromatic radiation are shown in Fig. 5. The dominant peak at 289.0 eV binding energy is attributed to the carbonate ion in calcite. At 5.2 ± 0.1 eV lower binding energy from the carbonate C 1s peak, a feature attributed to the adventitious C–H impurity can be observed. With the 20° take-off angle, this feature is of an almost comparable intensity with the carbonate C 1s line, while its intensity has been reduced to one tenth of the carbonate line in the case of the 60° take-off angle. The reduction in intensity shows that the peak originates from the surface. We shall discuss the origin of this chemical species in the next section. In addition, $K_{\alpha 3}$ and $K_{\alpha 4}$ satellites originating from the
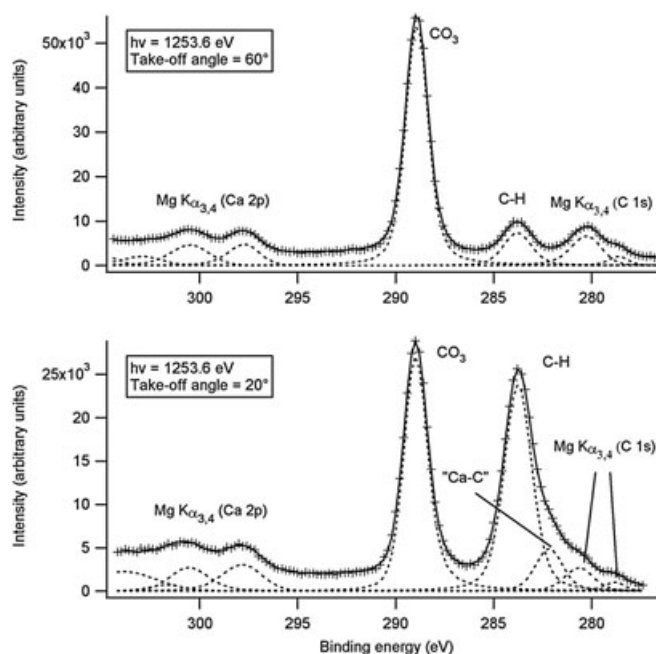

Figure 5. C 1s spectra of Iceland spar obtained with conventional XPS. Markers indicate raw data without background subtraction, dashed lines are the fitted individual components and the thin solid line is the sum of the dashed lines.

Ca 2p doublet and CO_3 peak are marked in the figure for both take-off angles. The FWHMs of the carbonate peaks are 1.3 eV (60°) and 1.4 eV (20°) indicating a possible surface component in the latter spectrum. Other reported FWHMs range from 1.1 to 1.8 eV.[19–21,25,38]

The peak seen in the lower (more surface sensitive) part of Fig. 5 at 6.9 eV lower binding energy from the C 1s line of CO_3 has been previously attributed to carbide (CaC_2).[40] Its existence is suggested to indicate beam-assisted interaction with the hydrocarbons found on the surface, because in the first (uppermost) spectrum of Fig. 6, which was obtained immediately after cleavage, no traces of either hydrocarbons or carbide can be seen. In Fig. 5, instead, hydrocarbons are abundant. The onset of the high binding energy side of both spectra is suggested to represent energy loss features of carbon.[41]
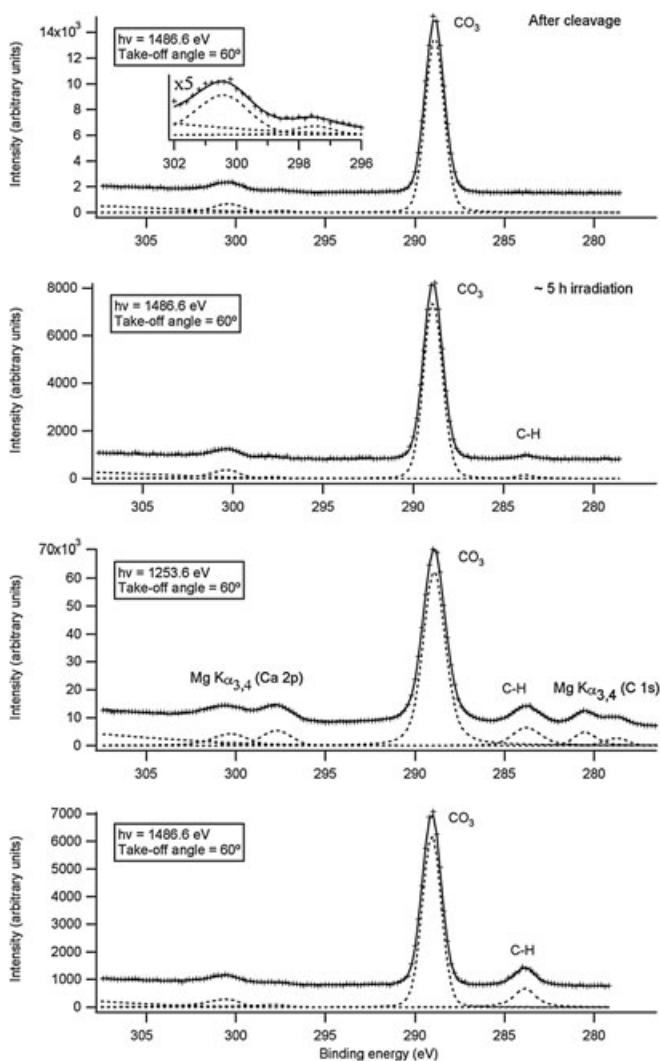

Figure 6. Conventional XPS spectra of C 1s obtained with monochromatic Al K$_\alpha$ ($h\nu$ = 1486.6 eV) and non-monochromatic Mg K$_\alpha$ ($h\nu$ = 1253.6 eV) radiation. A fivefold enlargement (of the vertical axis) of the satellite region is shown for the uppermost panel. The spectra were recorded in chronological order starting from the top; the uppermost spectrum was recorded immediately after cleavage, and the one below it after 5 h exposure to irradiation. The last two spectra were each recorded within an hour using the given radiation. Markers indicate raw data without background subtraction, dashed lines are the fitted individual components and the thin solid line is the sum of the dashed lines.

Changes in the C 1s spectrum

The influence of irradiation to the C 1s core level of a freshly cleaved sample was studied with a take-off angle of 60°. The obtained spectra are shown in Fig. 6. A fivefold enlargement (of the vertical axis) of the satellite region is inserted in the uppermost panel. In the uppermost (first) spectrum for which the measurement was completed approximately 60 min after cleavage, the C 1s peak originating from CO_3 is a single symmetrical peak. As discussed previously, carbide does not seem to be part of the calcite structure. At the high energy end of every spectrum in Fig. 6, there is an onset of a peak that represents energy loss features of carbon.[41] After 5 h exposure to Al K$_\alpha$ radiation, the measurement was repeated (second spectrum), and only a weak barely observable peak attributed to adventitious carbon (C–H) starts to appear at 5.1 eV lower binding energy.

When the X-ray source was switched to non-monochromatic Mg K$_\alpha$, the impurity peak (C–H) reached an intensity of approximately one tenth of the carbonate peak, and K$_{\alpha3}$ and K$_{\alpha4}$ satellites originating from CO_3 appeared. This radiation source was on for only about an hour, which is how long the measurement took. The fourth spectrum of the series uses again Al K$_\alpha$ excitation source for a recording time of an hour. As a result, the satellites have disappeared, but the impurity line still remains, with the same intensity ratio to the main CO_3 peak.

In the case of monochromatic radiation, two peaks are fitted for the binding energies of 297.5 and 300.4 eV (see the enlargement). The energy differences between these satellites and the CO_3 component are equal to 8.5 and 11.4 eV. As discussed previously and in the next section, these energies and the DFT calculations by Medeiros *et al.*[22] suggest that these features are bulk plasmons.

O 1s and Ca 2p spectra

Figure 4 represents O 1s and Ca 2p spectra of Iceland spar with fivefold enlargements (of the vertical axes) of the satellite regions. The acquisition of both spectra was completed within 50 min after cleavage. For O 1s, the peak with the highest binding energy that continues beyond the figure is interpreted to consist of extrinsic electron energy loss features. The three individual satellites are located at approximately 8.7, 11.0 and 16.1 eV higher binding energies than the main line. Again, we use the results of the DFT calculations of the dielectric function of calcite[22] in the interpretation. The first and the second features could represent bulk plasmons, because DFT calculations satisfy the conditions Re $\varepsilon(\omega_p) = 0$ and Im $\varepsilon(\omega_p)$ is at minimum for these energies, albeit there are differences of about 0.7 and −0.5 eV in the cases of first and second features, respectively. The first two features occurring at approximately the same binding energies have also been previously observed without a suggestion of their origin.[20] A second order plasmon might have partly contributed to the last feature, which is located approximately twice as far from the CO_3 peak as the first feature, which was interpreted to be a bulk plasmon.

The main O 1s peak originating from CO_3 is fitted with a single symmetric peak with FWHM equal to 1.4 eV, which is narrower than in most of the previous results.[19–21,25,38] Both Gopinath *et al.*[21] and Stipp and Hochella Jr.[19] suggest that their spectra include more than one type of chemical bonds contributing to the photoemission peak assigned to CO_3.

In the Ca 2p spectrum, the FWHMs of Ca 2p bulk and surface features are both equal to 1.3 eV; an SCLS of 0.6 eV is obtained.

Two satellites are located at 8.3 eV higher binding energies from the bulk doublet, which is in agreement with the previous interpretations of bulk plasmons. In this case, the measured binding energy region extends more to the high binding energy side than in the previous Ca 2p spectra in Figs 2 and 3. A minor feature located at the binding energy of 361.8 eV can therefore be seen. This feature allowed us to fit another doublet, which is represented by a different kind of dashed line (see the enlargement in Fig. 4). The used separation between the components was 3.6 eV, and the intensity ratio was 1:2. This smaller doublet is located at 11.5 eV higher binding energy than the Ca 2p doublet. Using the DFT calculations of Medeiros *et al.*,[22] and the interpretations presented previously [for Re $\varepsilon(\omega_p) = 0$ and a local minimum of Im $\varepsilon(\omega)$], we suggest that these peaks are also caused by the bulk plasmons. The Ca 2p spectrum was measured from the most contamination-free surface of this study so it seems unlikely that contamination would influence the SCLSs.
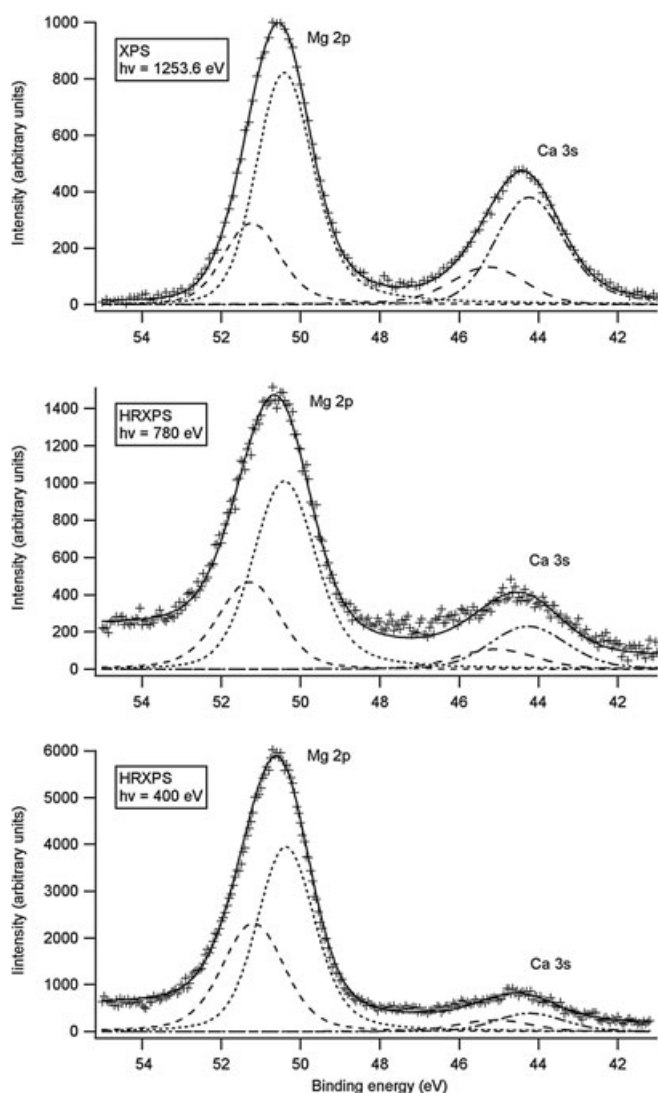

Figure 7. Mg 2p and Ca 3s spectra of dolomite for two different excitation energies of high-resolution XPS (HRXPS) and one spectrum obtained with conventional XPS. Markers indicate raw data without background subtraction, dashed lines are the fitted individual components and the thin solid line is the sum of the dashed lines. The electron take-off angle was 45°.

Polycrystalline dolomite

The total spectrum obtained with conventional XPS ($hv = 1253.6$ eV) from dolomite powder is shown in Fig. 1. Ca 2p, O 1s, Mg 2s and C 1s lines are marked in addition to silicon and aluminium originating from impurity minerals in the sample. Other impurity elements not marked on the figure include iron, fluorine and adventitious carbon.

Figure 7 shows Mg 2p and Ca 3s spectra of dolomite obtained with both conventional XPS and HRXPS. According to the authors' knowledge, only Gopinath *et al.*[21] and Hu *et al.*[42] have published these spectra for dolomite. The Mg 2p peaks in this study were fitted with a spin-orbit splitting of $\Delta_{s-o} = 0.28$ eV[43] and an intensity ratio of 1:2. The lifetime widths were fixed to be equal for both components, while the instrumental widths were allowed to change freely. The Mg 2p peak position (50.3 eV) was taken from the work of Hu *et al.*,[42] and used for the calibration of bulk Mg $2p_{3/2}$. An SCLS of 0.75 ± 0.05 eV was fitted for all Mg 2p and Ca 3s spectra, which sounds reasonable because both Mg and Ca are alkaline earth metals. This surface component is located on the high binding energy side of the main line as in the Ca 2p spectra of calcite. The fitting of two doublets (bulk and surface) for the Mg 2p peak is justified by the observation that a decrease in the energy of excitation radiation decreases the area ratio of the bulk peak to the surface peak and changes the shape of the total Mg 2p spectrum. The FWHMs of bulk originated Mg $2p_{3/2}$ peaks are equal to 1.7, 1.8 and 1.7 eV for photon energies of 1253.6, 780 and 400 eV, respectively.

Mg/Ca atomic concentration ratio

Figure 8 shows photoionisation cross section ratios for Mg 2p/Ca 3s taken from several sources. A clear consistency between them is observed. In addition, the ratio for the areas under the Mg 2p and Ca 3s curves is shown. Its similar shape indicates that peak areas are proportional to photoionisation cross sections. Therefore, it might be possible to estimate Mg/Ca atomic concentration by
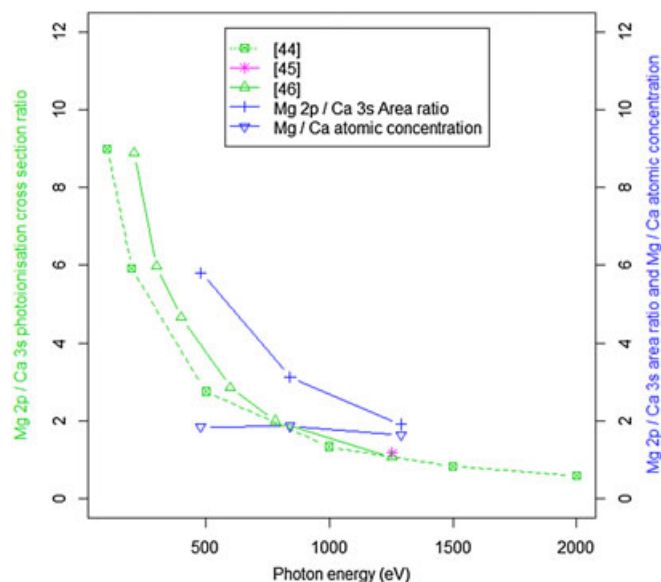

Figure 8. Mg 2p/Ca 3s photoionisation cross section ratios, Mg 2p/Ca 3s area ratio and Mg/Ca atomic concentration calculated using the area ratio and a cross section ratio.[46] The figure was compiled using R statistical software.[47]

dividing the area ratio by the ratio of the photoionisation cross sections of Mg 2p and Ca 3s, as represented in equation

$$\frac{C_{Mg}}{C_{ca}} = \frac{\frac{A_{Mg2p}}{A_{Ca3s}}}{\frac{\sigma_{Mg2p}}{\sigma_{Ca3s}}}, \quad (1)$$

where C_i is atomic concentration of element i in atomic %, A_j is area under the photoelectron peak j in counts and σ_k is photoionisation cross section in the case of photoelectron k in barns. Intensity of a peak is assumed to be proportional to the peak's area. The Mg/Ca atomic ratios were calculated using the photoionisation cross section data from the work of Yeh and Lindau[46] and plotted in Fig. 8. The ratios indicate that the dolomite sample has approximately twice as much magnesium compared with calcium independent of the excitation energy (degree of surface sensitivity). The constant Mg/Ca ratio further indicates that the cleavage has not left a layer of magnesium or calcium on top of the surface, because it would show up as surface enrichment. The attenuation length of the electrons should not have much influence on the area relation because the Mg 2p and Ca 3s peaks have approximately the same binding energies. However, the previous equation is only an approximation where photoionisation cross sections[46] were calculated for individual atoms, not for solid state matter. In addition, it has been pointed out that instrumental correction factors determined from $CaCl_2$ and $MgCl_2$ samples for the particular spectrometer should be used instead of calculated sensitivity factors.[42]

Previously, XPS has been used to obtain atomic concentrations for both calcite[19,21,25,38] and dolomite.[21,42] The published Mg/Ca atomic concentrations for dolomite surfaces are 1 (sample from Ward's Natural Science Est. Inc.[42]) and 1/3 (sample from Crystal Clays and Minerals, Rajasthan, India[21]). In addition, Gopinath et al.[21] discussed that the surface of their dolomite powder was more calcium rich than that of the subsurface layers. Unfortunately, no additional data is shown to support their suggestion of Mg/Ca ratio being a function of signal depth. The difference between these results and our study is obviously explained by the use of different kinds of samples from the solid-solution series of dolomites.

Conclusions

It has been shown that synchrotron-based XPS (HRXPS) is useful in studies of wide gap insulators calcite and dolomite. The obtained HRXPS results have been in good agreement with conventional XPS measurements. With successful neutralisation of the charges, it is possible that peaks obtained with HRXPS are narrower than those obtained with conventional XPS. SCLSs in Ca 2p spectra of calcite have been found to be very similar to those of dolomite, which were obtained from the Mg 2p spectra. Some satellite features in the Ca 2p, C 1s and O 1s spectra of calcite have been suggested to be bulk plasmons because of the agreement between our data and DFT calculations. A peak that was attributed to carbide (CaC_2) has been suggested to indicate beam assisted interaction with the hydrocarbons found on the surface.

Acknowledgements

References

[1] J. Cheng, J. Zhou, J. Liu, Z. Zhou, Z. Huang, X. Cao, X. Zhao, K. Cen, *Prog. Energy Combust. Sci.* **2003**, *29*, 381.

[2] R. A. Berner, A. C. Lasaga, R. M. Garrels, *Am. J. Sci.* **1983**, *283*, 641.

[3] J. W. Morse, R. S. Arvidson, *Earth-Sci. Rev.* **2002**, *58*, 51.

[4] S. Rode, N. Oyabu, K. Kobayashi, H. Yamada, A. Kühnle, *Langmuir* **2009**, *25*, 2850.

[5] J. Geyssant, in *Calcium Carbonate: from the Cretaceous Period into the 21st Century* (Eds: F. W. Tegethoff, J. Rohleder, E. Kroker), Birkhäuser Verlag, Basel, Switzerland, **2001**, pp. 1–52.

[6] H.-R. Wenk, A. Bulakh, *Minerals: Their Constitution and Origin*, Cambridge University Press, Cambridge, **2008**.

[7] B. Mason, L. G. Berry, *Elements of Mineralogy*, W. H. Freeman and Company, San Francisco, **1968**.

[8] J. O. Titiloye, N. H. de Leeuw, S. C. Parker, *Geochim. Cosmochim. Acta* **1998**, *62*, 2637.

[9] F. M. Hossain, B. Z. Dlugogorski, E. M. Kennedy, I. V. Belova, G. E. Murch, *Comput. Mater. Sci.* **2011**, *50*, 1037.

[10] C. C. Chusuei, D. W. Goodman, in *Encyclopedia of Physical Science and Technology* (Ed: R. A. Meyers), Elsevier B. V., ScienceDirect, **2004**, pp. 921–938.

[11] D. R. Baer, D. L. Blanchard, Jr., *Appl. Surf. Sci.* **1993**, *72*, 295.

[12] H. Gonska, H. J. Freund, G. Hohlneicher, *J. Electron Spectrosc. Relat. Phenom.* **1977**, *12*, 435.

[13] S. Oswald, S. Baunack, *Surf. Interface Anal.* **1977**, *25*, 942.

[14] B. J. Tielsch, J. E. Fulghum, *Surf. Interface Anal.* **1996**, *24*, 28.

[15] S. Mukjerhee, M. Mukherjee, *J. Electron Spectrosc. Relat. Phenom.* **2007**, *154*, 90.

[16] J. Cazaux, *J. Electron Spectrosc. Relat. Phenom.* **2010**, *178*, 357.

[17] H. W. Nesbitt, G. M. Bancroft, R. Davidson, N. S. McIntyre, A. R. Pratt, *Am. Mineral.* **2004**, *89*, 878.

[18] C. S. Doyle, T. Kendelewicz, X. Carrier, G. E. Brown Jr., *Surf. Rev. Lett.* **1999**, *6*, 1247.

[19] S. L. Stipp, M. F. Hochella Jr., *Geochim. Cosmochm. Acta* **1991**, *55*, 1723.

[20] D. R. Baer, J. F. Moulder, *Surf. Sci. Spectra* **1993**, *2*, 1.

[21] C. S. Gopinath, S. G. Hegde, A. V. Ramaswamy, S. Mahapatra, *Mater. Res. Bull* **2002**, *37*, 1323.

[22] S. K. Medeiros, E. L. Albuquerque, F. F. Maia Jr., E. W. S. Caetano, V. N. Freire, *J. Phys. D Appl. Phys.* **2007**, *40*, 5747.

[23] J. Moulder, D. Hook, *PHI Interface* **1997**, *17*, 1.

[24] E. Kukk, Spectral Analysis by Curve Fitting Macro Package /SPANCF/ 2000, available at: http://www.physics.utu.fi/en/department/ materials_research/materials_science/Fitting.html [Accessed on 2nd November 2012].

[25] L. Järvinen, J. A. Leiro, F. Bjondahl, C. Carletti, O. Eklund, *Surf. Interface Anal.* **2012**, *44*, 519.

[26] D. L. Blanchard Jr., D. R. Baer, *Surf. Sci.* **1992**, *276*, 27.

[27] M. O. Krause, J. H. Oliver, *J. Phys. Chem. Ref. Data* **1979**, *8*, 329.

[28] J. A. Leiro, M. H. Heinonen, *Phys. Rev. B* **1999**, *59*, 3265.

[29] A. J. Skinner, J. P. LaFemina, H. J. F. Jansen, *Am. Mineral.* **1994**, *79*, 205.

[30] R. J. Reeder, in *Reviews in Mineralogy vol. 11, Carbonates: Mineralogy and Chemistry* (Ed: R. J. Reeder), Mineralogical Society of America, Washington DC, **1983**, pp. 1–48.

[31] L. Cheng, N. C. Sturchio, J. C. Woicik, K. M. Kemner, P. F. Lyman, M. J. Bedzyk, *Surf. Sci.* **1998**, *415*, L976.

[32] P. H. Citrin, G. K. Wertheim, Y. Baer, *Phys. Rev. Lett.* **1978**, *41*, 1425.

[33] K. C. Prince, G. Paolucci, V. Cháb, M. Surman, A. M. Bradshaw, *Surf. Sci. Lett.* **1988**, *206*, L871.

[34] W. Mönch, *Solid State Commun.* **1986**, *58*, 215.

[35] B. W. Veal, A. P. Paulikas, *Phys. Rev. B* **1985**, *31*, 5399.

[36] R. A. Heaton, C. C. Lin, *Phys. Rev. B* **1980**, *22*, 3629.

[37] J. Leiro, E. Minni, E. Suoninen, *J. Phys. F: Met. Phys.* **1983**, *13*, 215.

[38] M. Ni, B. D. Ratner, *Surf. Interface Anal.* **2008**, *40*, 1356.

[39] A. B. Christie, I. Sutherland, J. M. Walls, *Vacuum* **1981**, *31*, 513.

[40] J. Moulder, W. Stickle, P. Sobol, K. Bomben, *Handbook of X-ray Photoelectron Spectroscopy*, Perkin-Elmer, Eden Prairie, MN, **1992**.

[41] J. A. Leiro, M. H. Heinonen, T. Laiho, I. G. Batirev, *J. Electron Spectrosc. Relat. Phenom.* **2003**, *128*, 205.

[42] X. Hu, P. Joshi, S. M. Mukhopadhyay, S. R. Higgins, *Geochim. Cosmochim. Acta* **2006**, *70*, 3342.

[43] V. Karpus, A. Suchodolskis, U. O. Karlsson, G. Le Lay, L. Giovanelli, W. Assmus, S. Brühne, E. Uhrig, *Appl. Surf. Sci.* **2006**, *2252*, 5411.

[44] M. B. Trzhaskovskaya, V. I. Nefedov, V. G. Yarzhemsky, *At. Data Nucl. Data Tables* **2001**, *77*, 97.

[45] J. H. Scofield, *J. Electron Spectrosc. Relat. Phenom.* **1976**, *8*, 129.

[46] J. J. Yeh, I. Lindau, *At. Data Nucl. Data Tables* **1985**, *32*, 1.

[47] R Core Team. R: A language and environment for statistical Computing, R Foundation for Statistical Computing, Vienna, Austria, **2012**.